Spectral super-resolution spectroscopy using a random laser

Spectral super-resolution spectroscopy using a random laser

Alice Boschetti*[1], Andrea Taschin[1,2], Paolo Bartolini[1], Anjani Kumar Tiwari[3], Lorenzo Pattelli[1,4], Renato Torre[1,5], Diederik S. Wiersma*[1,4,5]

[1]European Laboratory for Non-Linear Spectroscopy (LENS) / University of Florence, Via Nello Carrara, 1 - 50019 Sesto Fiorentino, Italia

[2]ENEA, Centro Ricerche Frascati, Via E. Fermi, 45 – 00044, Frascati, Italia

[3]Department of Physics, Indian Institute of Technology Kanpur, 208016 Kanpur, India

[4]Istituto Nazionale di Ricerca Metrologica (INRIM), Strada delle Cacce, 91 – 10135 Torino, Italia

[5]Department of Physics, University of Florence, Via Sansone, 1 – 50019 Sesto Fiorentino, Italia

*email: boschetti@lens.unifi.it, wiersma@lens.unifi.it

Abstract

Super-resolution microscopy refers to a powerful set of imaging techniques that overcome the diffraction limit. Some of these techniques, of which the importance was emphasized by the 2014 Nobel Prize for chemistry, are based on the clever concept of image reconstruction by spatially sparse sampling. Here, we introduce the concept of super-resolution spectroscopy based on sparse sampling in the frequency domain, and show that this can be naturally achieved using a random laser source. In its chaotic regime, the emission spectrum of a random laser features sharp spikes at uncorrelated frequencies that are sparsely distributed over the emission bandwidth. These narrow lasing modes probe stochastically the spectral response of a sample, allowing to

reconstruct it with a resolution exceeding that of the spectrometer. We envision that the proposed technique will inspire a new generation of simple and cheap, high-resolution spectroscopy tools with reduced footprint.

In general, the concept of super-resolution refers to the possibility to obtain a higher quality digital reconstruction of a detected signal, using sets of low-resolution measurements. In the field of optics, various methods have been proposed for super-resolution imaging, with the aim of obtaining a resolution that is beyond the diffraction limit[1,2,3,4,5]. Super-resolution microscopy based on single molecule localization has undergone a rapid development in recent years[6,7,8]. It relies on the principle of repetitive and spatially sparse activation of point-like sources inside the sample. Each point source generates a blurred disk-shape whose centroid can be obtained with sub-pixel resolution by a fitting procedure. While one image only contains the information on a few points of the desired object, accumulating a large amount of such points allows to reconstruct the entire image at a resolution that is much higher than that of the imaging system.

Some attempts have been undertaken to improve the resolution of spectral measurements, for instance, by making use of known information regarding the source. Out of these, a few noteworthy approaches include the analysis of spectra that can be assumed to have a compact representation[9] or the extension of a dataset in the Fourier domain to improve resolution of the target signal[10].

In this work, we wish to introduce a new idea in spectroscopy, namely that of sparse sampling in the frequency domain, using random lasers as light source. The purpose is to achieve super-resolution in the spectroscopic characterization of samples; that is, to obtain a characterization with spectral features that are finer than the nominal resolution of the spectrometer. Below we will explain the idea and discuss various aspects of its implementation. We will start with a numerical simulation to test the concept and then show an experimental realization where the spectrum of a custom-made etalon filter is reconstructed as an example.

It is well-known that the resolution of a spectrometer can be defined by the Rayleigh criterion[11] i.e., its ability to identify two adjacent spectral lines. This is strictly connected with the spectral “instrumental line profile”, $I(\lambda)$, corresponding to the spectral line measured by a detector at the output slit if a “monochromatic field” is focused at the spectrometer entrance slit. The full width half maximum (FWHM) of $I(\lambda)$ defines the

spectrometer resolution. This implies that any spectrum S(λ), analysed by the spectrometer, is the result of the convolution of the real spectrum $S_0(\lambda)$ with the instrumental line profile I(λ):

$$S(\lambda)=S_0(\lambda)\otimes I(\lambda). \qquad [\text{eq.1}]$$

The shape of I(λ) depends both on the properties of the spectrometer and the detector.

To explore the possibility of using a random laser source for super-resolution spectroscopy, let us consider the example of a low-finesse Fabry Perot (FP) characterized by a free spectral range (FSR) well below the spectral resolution of a measuring apparatus (FWHM= 4.9×FSR). We will first consider a numerical simulation of this system and later in the paper report on its experimental characterization, using, in both cases, the concept of sparse sampling in the spectral domain with a random laser as light source.

A numeric example

In Figure 1, the outline of the setup is shown as modelled in the numerical simulation. This outline also serves to illustrate the idea more in detail. Two types of light sources have been considered: a random laser (blue in the figure) and a regular lamp as comparison (yellow in the figure). The transmission of the etalon is measured versus frequency, using a low resolution spectrometer (indicated in green, together with its (broad) spectral response function). In the yellow graph (panel b) the optical response is shown when the sample is illuminated with an ideal Gaussian-shaped broadband illumination source. Due to the convolution of the transmission spectrum of the sample with the (broad) instrumental response function of the spectrometer, the Fabry-Perot fringes disappear almost completely. From a mathematical point of view, by knowing I(λ) exactly for an ideal delta-like source, it would still be possible to recover the original signal using a deconvolution operation. However, this is unfeasible in practice due to the finite noise level of any real measurement, and it is in fact already challenging even in this simulated case due to numerical instability of deconvolution, which is highly susceptible to finite precision of computed functions[12,13].

Here, we will show that it is possible to retrieve the target transmission function by performing a sparse frequency sampling, just as sparse spatial sampling allows to retrieve an image in super-resolution microscopy. More precisely, we will use a random laser in the chaotic regime as the illumination source, taking advantage of the inherent spectral separation of a typical random laser emission spectrum. Random lasers are laser

sources using a disordered gain medium, with no external cavity[14,15]. The term 'random lasing' refers to the fact that its modes are disordered in nature. The physics behind random lasing is quite rich[14,16]. For instance, the number of modes is typically huge and a large amount of modes can be overlapping both in space and frequency. This leads to strong mode coupling and a broad parameter regime in which the output is chaotic[17]. At each random laser shot only a few modes actually reach threshold leading to the typical random laser emission spectrum that consist of a few narrow 'spikes' well-separated from each other. Additionally, in the chaotic regime of operation, the emission spectrum of each random laser pulse is completely uncorrelated from the previous pulse. Overall, these properties make random lasers an ideal class of sources for sparse sampling in the frequency domain.

By recording peak amplitudes and frequencies for the most prominent peaks through a series of chaotic spectra, it is possible to reconstruct the super-resolved transmission function of a sample with its original contrast. Typically, having only a few prominent peaks for each lasing spectrum, it is possible to retrieve their centre frequency with high, sub-pixel precision. Once a large ensemble (in the order of a few thousand depending on the desired level of signal-to-noise ratio) of lasing peaks has been collected, plotting their amplitudes as a function of frequency provides a reconstruction of the super-resolved target spectrum, free of deconvolution artefacts.

Numerical simulations have been performed on large sets of computer generated random laser spectra to test the concept and to understand its ideal parameters of operation (including the number of lasing modes, their optimal spacing, and the number of spectra over which one should average). In Figure 1d, a few of the numerically simulated transmission spectra have been plotted. In each transmission curve, one can identify isolated broadened peaks of which the centre can be identified. Each of such peaks then provides one point in the reconstruction of the target spectrum. In the bottom panel of Figure 1, the reconstructed spectrum is shown using a total of 10^4 single shot random laser spectra with a simulated noise level of 0.1% of the maximum of the fluorescence curve. For comparison, we also show the result for a broadband source like a regular lamp, using the same parameters. While nearly all information is lost using the broadband source, random laser illumination allows to reconstruct the target spectrum with very good precision. Regular deconvolution is very sensitive to small noise fluctuations – which are amplified in the reconstructed spectrum. The statistical reconstruction using a random laser is much more stable and successfully retrieves the original

Fabry-Perot contrast and spectral pattern – especially in the central region where the random laser statistics is larger. We have performed a broad range of similar simulations and found that random laser based super-resolved spectral reconstruction can be applied nearly arbitrarily, for a wide range of apparatus response functions and target transmission spectra.

Experimental results

In order to test our ideas in practice, we performed an experimental analysis, again using a Fabry-Perot as an example. The etalon was realized with a free spectral range of 0.3 THz and a maximum transmission contrast of 32%. A spectrometer was used with a resolution that did not allow to resolve the interference fringes of the etalon (FWHM= 2.8·FSR). The analysis was performed with a random laser and with a regular lamp for comparison. The outline of the experimental setup is sketched in Figure 2. A microscope objective is used both to focus the pump laser and to collect the random laser signal. The random laser emission is split by a 50:50 beam splitter into two beams: a reference signal – which is directly coupled to one entrance of a multimodal fibre bundle, and a probe signal passing through the sample before being focused on the other fibre entrance. A magnified image of the two fibre ends is reproduced on the entrance slit of a monochromator, and a CCD camera finally records the image reproduced on its output focal plane. (See Methods section for more details.)

The random laser was realized by suspending ZnO nanoparticles in a solution of Rhodamine 6G and ethanol (see Methods for technical details). A frequency doubled Nd:YAG laser was used to optically pump the random laser. Lasing was observed above a threshold of 0.5 μJ energy per pump pulse. The laser was operated above threshold but still well within its chaotic regime of operation, characterized by Lévy-distributed intensity fluctuations[18,19]. Single-shot emission spectra are found to be entirely uncorrelated, with narrow peaks appearing at independent frequencies. An example of such an emission spectrum is shown in Figure 2b, while more examples can be found in the supplementary information. The output of this random laser was then used as a source to characterize the FP, whose transmission function is shown in Figure 2c as measured independently with a high-resolution spectrometer with a linewidth 0.13 THz.

Figure 2d reports the transmission spectrum of a single random laser shot as measured by the low-resolution spectrometer. The sample modulates the intensity of the probe signal with respect to the reference,

but, as expected, the visibility of the FP transfer function is completely lost even in the fluorescence background. Nonetheless, information on the transmission function of the sample is still contained in the relative heights of the peaks in the measured spectrum and can be retrieved by analysing a large number of random laser shots. For that purpose, the centre of each peak should be determined accurately, as well as the modulation of the peak height by the sample (obtained by comparing the transmission through the sample with the reference beam).

The steps of this statistical analysis are shown in Figure 3. A set of 4000 single-shot random laser spectra is collected, each of them producing a double trace. All traces contain both the transmitted signal (bottom) as well as its respective reference signal (top). For each shot, isolated random laser modes are selected by an algorithm that identifies bright disks within a certain diameter range as defined by the spectral resolution of the spectrometer. For each disk selected in the transmission signal, we compute its intensity by integrating over the disk area and normalizing it by the integral of the respective disk found in the reference signal. The reference signal is also used to determine the central frequency of the unaltered peak in order to avoid apparent frequency shifts that could be possibly induced by steep modulations of the transmission function.

Discussion

The procedure of sparse sampling in the frequency domain allows to reconstruct the transmission function of the sample. We should note here that by “sparse sampling” we simply refer to a minimum average spectral separation between the lasing peaks. Seeking this condition is an important factor for the efficiency of the reconstruction technique as it can reduce drastically the probability of having two almost-degenerate lasing modes during the same laser shot, which would go unresolved by the spectrometer (See SI). Frequency sparsity is an intrinsic characteristic of random laser emission spectra and it can be exploited to achieve a sampling of a transmission function unaffected from convolution effects. By acquiring a sufficiently large statistics on the transmitted frequency positions and amplitudes, the whole spectrum can be reconstructed, as we show for our exemplary test case in Figure 4a.

One can clearly see that the transmission function of the FP etalon is reconstructed with all its relevant features. For comparison, when the transmission spectrum is measured using a standard lamp as light source, the etalon transmission function cannot be retrieved even when averaging over the same amount of spectra to

reduce measurement noise (Fig. 4b). The effectiveness of the method is further highlighted by analysing the results in the Fourier domain. The periodicity of the transmission function of the FP etalon is clearly retrieved when using the random laser, while it is lost in the lamp measurements (See Figs. 4c and 4d).

In conclusion, we have shown that it is possible to perform super-resolution *spectroscopy* exploiting the intrinsic features of random laser emission for spectral sparse sampling – analogously to sparse sampling in super-resolution *microscopy*. We have introduced the idea, analysed its parameter space of operation using numerical calculations, and performed an experimental demonstration on a test etalon sample. Our results show that it is possible to retrieve spectral features of a transfer function below the resolution limit imposed by the spectrometer. As confirmed by our analysis both in direct and reciprocal space, our method delivers accurate reconstruction despite minimal algorithm optimization and the moderate size of the statistical ensemble of random laser peaks used.

We have shown a ~3 spectral enhancement factor, but in principle the method can be adapted to spectrometers whose response function is arbitrary in width and shape, which poses no upper limit to the effective enhancement that can be achieved. In absolute terms, an ultimate resolution limit is represented by the linewidth of the individual random laser modes (which, in our case, was around 0.19 THz). Random lasing modes with much narrower widths can be obtained, e.g., by spatially tailoring the pumping light [20]. Additionally, compressive sensing methods should be straightforwardly applicable to the reconstruction technique in order to reduce the number of spectra required to obtain a certain signal-to-noise level[21,22].

Most importantly, our approach relies entirely on the chaotic variation of the illumination spectrum to ensure narrow line widths and a uniform sampling over the emission band, and hence does not require any stabilization of the lasing source – which is otherwise critical in other high-resolution approaches such as frequency comb spectroscopy [23], nor it requires an exact knowledge of the instrumental spectral response as in typical deconvolution algorithms.

Quite interesting, the distinctive features of random laser emission – namely their huge variety of modes, their chaotic behaviour and naturally sparse population – make these illumination sources ideal candidates for this super-resolved stochastic reconstruction approach. We believe that the concept introduced in this paper can possibly lead to a new generation of high-resolution spectral analysis providing a small footprint, low-cost

alternative to the use of more expensive broadband-tunable narrow line lasers. Our technique is based on a general principle and can be straightforwardly replicated in different wavelength regions ranging from the UV to the mid-infrared, where random laser sources are already available[24,25,26,27,28,29]. Taking advantage of more recent electrically-pumped random lasing schemes holds promise to further extend the applicability of our approach, making it making it more energy-efficient, compatible with CMOS technology and suitable for large-scale production and integration in devices[30,31].

Data availability

The data that support the plots within this paper and other findings of this study are available from the corresponding author upon reasonable request.

Bibliography

1. Betzig, E., Trautman, J. K., Harris, T. D., Weiner, J. S. & Kostelak, R. L. Breaking the diffraction barrier: optical microscopy on a nanometric scale. *Science* **251**, 1468–70 (1991).
2. Hell, S. W. & Wichmann, J. Breaking the diffraction resolution limit by stimulated emission: stimulated-emission-depletion fluorescence microscopy. *Opt. Lett.* **19**, 780 (1994).
3. Gazit, S., Szameit, A., Eldar, Y. C. & Segev, M. Super-resolution and reconstruction of sparse sub-wavelength images. *Opt. Express* **17**, 23920 (2009).
4. Szameit, A. *et al.* Sparsity-based single-shot subwavelength coherent diffractive imaging. *Nat. Mater.* **11**, 455–459 (2012).
5. Huang, F. M. & Zheludev, N. I. Super-Resolution without Evanescent Waves. *Nano Lett.* **9**, 1249–1254 (2009).
6. Rust, M. J., Bates, M. & Zhuang, X. Sub-diffraction-limit imaging by stochastic optical reconstruction microscopy (STORM). *Nat. Methods* **3**, 793–796 (2006).
7. Hess, S. T., Girirajan, T. P. K. & Mason, M. D. Ultra-High Resolution Imaging by Fluorescence Photoactivation Localization Microscopy. *Biophys. J.* **91**, 4258–4272 (2006).

8. Betzig, E. *et al.* Imaging intracellular fluorescent proteins at nanometer resolution. *Science* **313**, 1642–5 (2006).

9. Kawata, S., Minami, K. & Minami, S. Superresolution of Fourier transform spectroscopy data by the maximum entropy method. *Appl. Opt.* **22**, 3593 (1983).

10. Sidorenko, P. *et al.* Super-resolution spectroscopy by compact representation. in *Frontiers in Optics 2012/Laser Science XXVIII* FM3F.5 (OSA, 2012). doi:10.1364/FIO.2012.FM3F.5

11. Pedrotti, F. L., & Pedrotti, L. S. *Introduction to optics*. (Prentice-Hall, 1987).

12. Blass, W. E. & Halsey, G. W. *Deconvolution of absorption spectra*. (Academic Press, 1981).

13. Mou-Yan, Z. & Unbehauen, R. A deconvolution method for spectroscopy. *Meas. Sci. Technol.* **6**, 482–487 (1995).

14. Wiersma, D. S. The physics and applications of random lasers. *Nat. Phys.* **4**, 359–367 (2008).

15. Liu, J. *et al.* Random nanolasing in the Anderson localized regime. *Nat. Nanotechnol.* **9**, 285–289 (2014).

16. Cao, H., Chriki, R., Bittner, S., Friesem, A. A. & Davidson, N. Complex lasers with controllable coherence. *Nat. Rev. Phys.* **1**, 156–168 (2019).

17. Uppu, R., Tiwari, A. K. & Mujumdar, S. Identification of statistical regimes and crossovers in coherent random laser emission. *Opt. Lett.* **37**, 662 (2012).

18. Araújo, C., Gomes, A. & Raposo, E. Lévy Statistics and the Glassy Behavior of Light in Random Fiber Lasers. *Appl. Sci.* **7**, 644 (2017).

19. Sharma, D., Ramachandran, H. & Kumar, N. Lévy statistics of emission from a novel random amplifying medium: an optical realization of the Arrhenius cascade. *Opt. Lett.* **31**, 1806 (2006).

20. Bachelard, N., Gigan, S., Noblin, X. & Sebbah, P. Adaptive pumping for spectral control of random lasers. *Nat. Phys.* **10**, 426–431 (2014).

21. Zhu, L., Zhang, W., Elnatan, D. & Huang, B. Faster STORM using compressed sensing. *Nat. Methods* **9**, 721–723 (2012).

22. Katz, O., Bromberg, Y. & Silberberg, Y. Compressive ghost imaging. *Appl. Phys. Lett.* **95**, 131110 (2009).

23. Picqué, N. & Hänsch, T. W. Frequency comb spectroscopy. *Nat. Photonics* **13**, 146–157 (2019).

24. Liang, H. K. *et al.* Electrically Pumped Mid-Infrared Random Lasers. *Adv. Mater.* **25**, 6859–6863 (2013).

25. Ni, P. N. *et al.* Fabry-Perot resonance enhanced electrically pumped random lasing from ZnO films.

Appl. Phys. Lett. **107**, 231108 (2015).

26. Liu, X.-Y., Shan, C.-X., Wang, S.-P., Zhang, Z.-Z. & Shen, D.-Z. Electrically pumped random lasers fabricated from ZnO nanowire arrays. *Nanoscale* **4**, 2843 (2012).

27. Yu, S. F. Electrically pumped random lasers. *J. Phys. D. Appl. Phys.* **48**, 483001 (2015).

28. Chu, S., Olmedo, M., Yang, Z., Kong, J. & Liu, J. Electrically pumped ultraviolet ZnO diode lasers on Si. *Appl. Phys. Lett.* **93**, 181106 (2008).

29. Ma, X., Chen, P., Li, D., Zhang, Y. & Yang, D. Electrically pumped ZnO film ultraviolet random lasers on silicon substrate. *Appl. Phys. Lett.* **91**, 251109 (2007).

30. Ma, X., Li, Y. & Yang, D. Electrically pumped random laser device based on dual SiO2-ZnO structure and preparation method and application thereof. (2012).

31. Qiao, Q*. et al.* Surface plasmon enhanced electrically pumped random lasers. *Nanoscale* **5**, 513–517 (2013).

32. Poison, R. C., Raikh, M. E. & Vardeny, Z. V. Universal properties of random lasers. *IEEE J. Sel. Top. Quantum Electron.* **9**, 120–123 (2003).

33. Frolov, S. V, Vardeny, Z. V, Yoshino, K., Zakhidov, A. & Baughman, R. H. *Stimulated emission in high-gain organic media*.

Acknowledgements

We gratefully acknowledge Stefano Caporali for his assistance with sputter deposition of Fabry-Perot mirrors and Luca Mariani for advice on the optical fibre elements. We acknowledge Marco De Pas, Alessandro Montori and Mauro Giuntini for their assistance in the set-up of electronics and Riccardo Ballerini and Ahmed Hajeb for the realizations of mechanical elements.

This research was funded by Ente Cassa di Risparmio Firenze (2016-0866), Ministero dell'Istruzione dell'Università e della Ricerca Italiano (PRIN2017-2017Z55KCW), European Community by Laserlab-Europe (H2020 EC-GA-654148) and PATHOS EU H2020 FET-OPEN grant no. 828946.

Contributions

A.B, A.T, P.B, L.P, A.K.T, R.T and D.W conceived the experiment, A.B., A.T. and P.B. conducted the experiment and analysed the results. A.B, A.T, L.P, A.K.T, R.T and D.W wrote the main manuscript text and A.B. prepared

the figures. All authors reviewed the manuscript.

Corresponding author

Correspondence to Diederik S. Wiersma and Alice Boschetti.

Competing Interest

The experimental apparatus and the analysis method are currently under patent filing.

Figure 1

Numerical demonstration of super-resolved spectroscopy.

a) A light source (broadband source or random laser) is used to illuminate a test sample (here a Fabry-Perot (FP)), its transmission spectrum being measured using a spectrometer (S) with a large point spread function (inset) and a linear camera (C). The numerical transmission function of the low finesse FP approximates a sinusoid with a free spectral range of 125 GHz.

b) Average of 10^4 numerical broadband transmission spectra of the Fabry-Perot test sample. The target transmission function is almost completely hidden by noise fluctuations and convolution with the broad instrumental response.

c) Spectral reconstruction obtained by direct deconvolution of the average broadband spectrum using the exact point spread function of the spectrometer (inset of panel a). The target response function is indicated by a grey line (as measured by the camera with a spectral resolution of FWHM=4.9·FSR). Deconvolution fails to retrieve the original response, showing spurious amplitude modulations and high-frequency oscillations.

d) Exemplary set of simulated transmission spectra obtained by illuminating the sample with single random laser shots, as measured by the low-resolution setup (blue). The original illumination spectra (dark blue) exhibit narrow lasing lines over the active medium fluorescence curve.

e) Spectral reconstruction obtained using the method introduced in this paper, using 10^4 single shot random laser spectra. On average, the original contrast of the Fabry-Perot is correctly restored, as well as its free spectral range.

Figure 2

Experimental apparatus for super-resolved spectroscopy.

a) The random laser source (RL) is optically excited by a pulsed pump laser (LS) focused using a 10x microscope objective. The same objective collimates the backscattered signal while an interference filter blocks back-reflected pump light. A 50:50 beam splitter (BS) sends a reference signal to a first multimode fibre, while the probe passes through the sample (in this case a Fabry-Perot filter (FP)) before being focused to a second fibre. The two fibre cores are bundled together and simultaneously focused at the entrance of the spectrometer (S) so that their output can be collected by the same detector (C).

b) Illustrative single-shot emission spectrum from the random laser source characterized independently with high spectral resolution.

c) Transmission curve of the investigated Fabry-Perot sample, as measured independently using a high-resolution spectrometer and a broadband lamp.

d) Illustrative random laser single-shot measured with the experimental scheme of the panel (a) using a low resolution spectrometer. The transmission spectrum (cyan curve) is compared to its respective reference spectrum (light blue curve). Inset shows the measured instrumental response of the low-resolution spectrometer.

Figure 3

Low-resolution peak selection.

Exemplary low-resolution spectra measured by the CMOS camera under random laser illumination. The top and bottom rows in each frame correspond to the reference and transmitted signal, respectively. An algorithm finds the most intense, non-overlapping circles within a fixed diameter range.

Each shot allows to reconstruct a few points of the target function.

Figure 4

Experimental demonstration of super-resolved spectroscopy.

a) Transmission curve obtained by sparse sampling using the random laser. The target transmission function is well reproduced exhibiting both its high- and low-frequency modulations, including its slow background slope (cfr. Fig. 2c).

b) Transmission curve as obtained with a common lamp for comparison. As expected, the transmission function of the Fabry-Perot etalon is lost due to convolution with the instrumental response function. c-d) Fourier transform of a-b), showing a prominent peak corresponding to the inverse of the etalon free spectral range, which is only visible in the case of our frequency-sparse sampling approach.

Methods

Random laser

A random laser is typically composed of a gain medium mixed with nanoparticles acting as scattering elements. In a random laser there is no optical cavity in the traditional sense and the feedback mechanism needed for lasing is provided by multiple scattering. Due to the disordered arrangement of the scattering medium, laser emission from a random laser is typically characterized by very complex spectral features.

Few technical points need to be considered in order to achieve super-resolved spectral measurements. First, the random laser source should exhibit, on average, a suitable distribution of chaotic lasing modes with few intense peaks sparsely distributed with uniform probability over the emission spectrum. Secondly, the emission spectrum of each lasing shot should be uncorrelated to the other shots (chaotic regime of operation). These requirements can be easily fulfilled by adjusting the pump energy and the excitation volume, representing a common mode of operation of a random laser.

In particular, varying the excitation volume allows to tune the average number of modes that go above threshold at each pump event[32-33], with a smaller volume (i.e., tighter pump lasing focusing) corresponding to

a sparser population of peaks over the gain bandwidth. The number of peaks should be such that the chance of observing two overlapping peaks can be neglected.

The random laser sample is made of a colloidal suspension of ZnO nanoparticles (10^{12} particles per cm^3, average particle diameter 200 nm) in a 5 mM solution of Rhodamine 6G dissolved in ethanol. The gain medium is optically pumped with a frequency-doubled pulsed Nd:YAG laser system (Ekspla, Mod. PL2143A), emitting pulses at 532 nm wavelength with a duration of 20 ps and a repetition rate of 10 Hz. We have determined for this system a random lasing threshold of about 0.5μJ per pulse, based on mode competition and gain depletion. The chaotic lasing regime, characterized by shot-to-shot uncorrelated, narrow lasing modes, is obtained for a pumping condition just above threshold[17].

Test sample

The low finesse Fabry-Perot (FP) test sample has been fabricated by sputter-coating a few nm of gold on the uncoated facets of two IR flat mirrors, resulting in a reflectivity of about 30%. The distance between the two mirrors was set so to obtain a free spectral range of 0.3 THz, corresponding to the finest FP modulation, optically characterized with a higher resolution monochromator (Chromex, mod. 250is entrance slit of 20 μm, 600 grooves/mm grating) coupled to a digital camera (Thorlabs, mod. DCC1240C, 1280×1024 pixel, 5.3 μm pixel size). The maximum transmission contrast through the custom-made etalon, $(I_{max}-I_{min})/I_{max}$, is equal to 32% as measured using the incandescent lamp.

Experimental setup

The experimental set-up is shown schematically in Figure 2. The pump beam is collimated to a diameter of 8 mm to match the entrance pupil of a 10× microscope objective (NA 0.3, effective focal length 18 mm). The objective focuses the pump beam to a 3 μm spot size on the surface of the random laser sample. The same objective collects the random laser emission which is then divided using a beam splitter into a reference beam and a probe beam. The reference is directly focused by a lens (*f*=50 mm) into one of the two entrances of a multimodal fibre bundle (fibre diameters 50 μm). The probe beam passes through the test sample and is then focused by a lens (*f*=50 mm) at the other fibre entrance. The two fibre outputs (separated by 85 μm) are focused on the entrance slit of the monochromator and collected by the digital camera, synchronized with the pump pulse. The resolution of the spectrometer can be tuned from an instrumental response of FWHM=0.13

391 THz to 0.83 THz by changing the input slit aperture from 20 μm to completely open. In the latter case, the
392 actual resolution is determined by the fibre output size (50 μm) and the entrance optics (3× magnification),
393 resulting in an effective illuminated aperture of 150 μm at the focal plane of the monochromator. This FWHM
394 corresponds to 2.8·FSR, and it is not sufficient to spectrally resolve the transmission function of the Fabry-
395 Perot test sample. The latter configuration has been used to demonstrate our super-resolution method and
396 reconstruct the transmission function of the test sample using the random laser source.
397

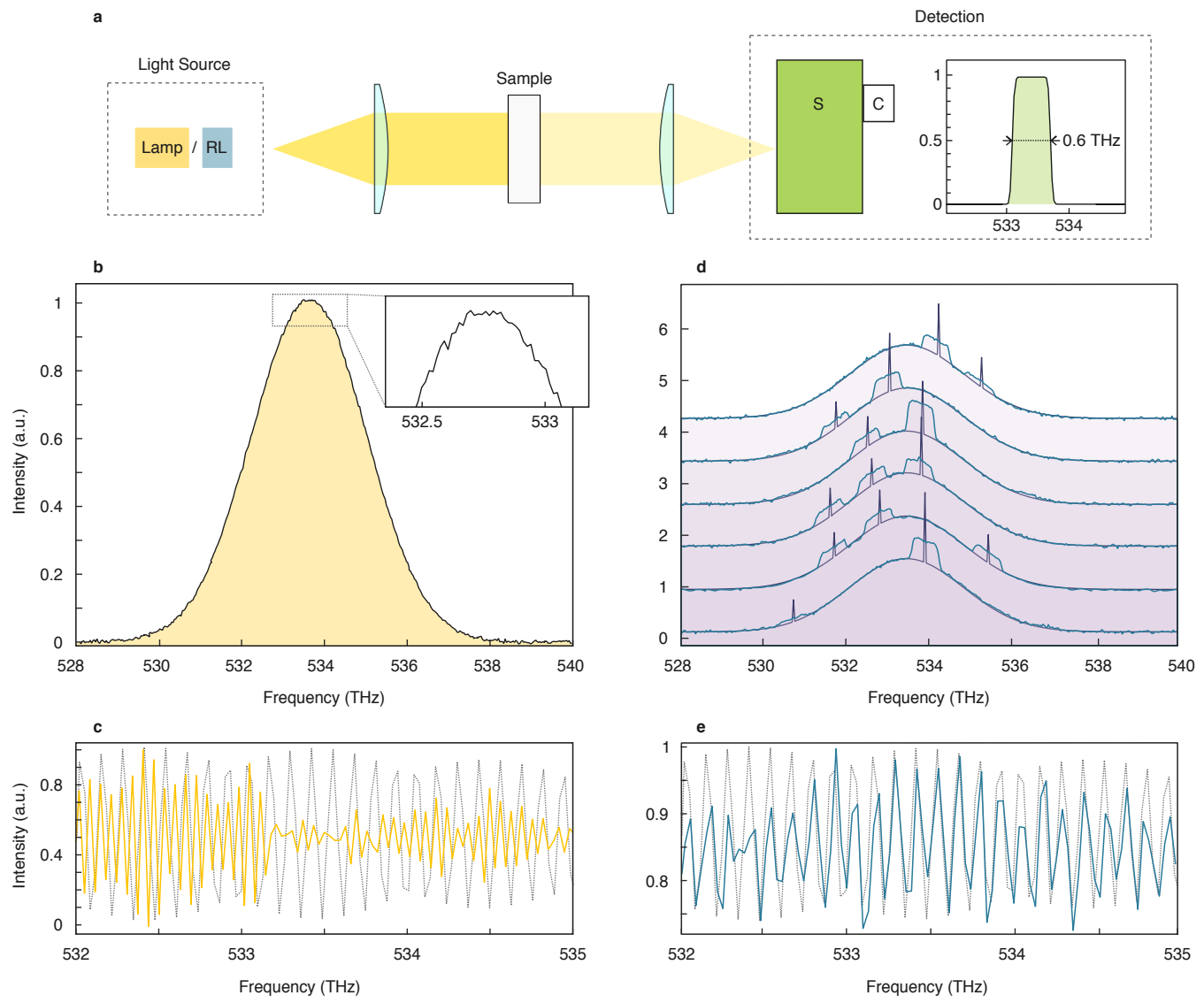
a
Light Source
Lamp / RL
Sample
Detection
S
C
1
0.5
0
0.6 THz
533
534
b
Intensity (a.u.)
1
0.8
0.6
0.4
0.2
0
532.5
533
528
530
532
534
536
538
540
Frequency (THz)
d
6
5
4
3
2
1
0
528
530
532
534
536
538
540
Frequency (THz)
c
Intensity (a.u.)
0.8
0.4
0
532
533
534
535
Frequency (THz)
e
1
0.9
0.8
532
533
534
535
Frequency (THz)

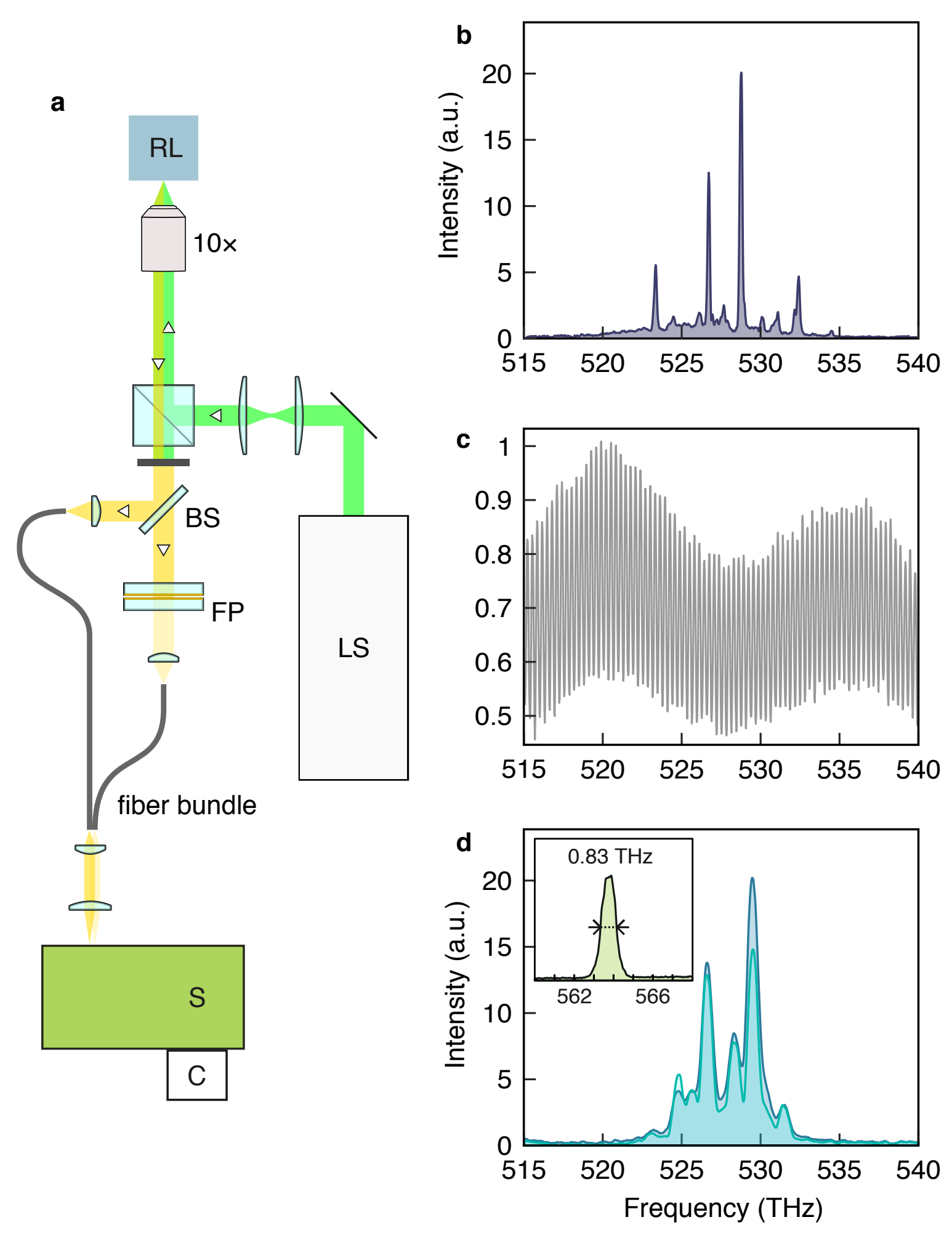
a
RL
10×
BS
FP
LS
fiber bundle
S
C
b
Intensity (a.u.)
0
5
10
15
20
515
520
525
530
535
540
c
0.5
0.6
0.7
0.8
0.9
1
d
0.83 THz
562
566
Frequency (THz)

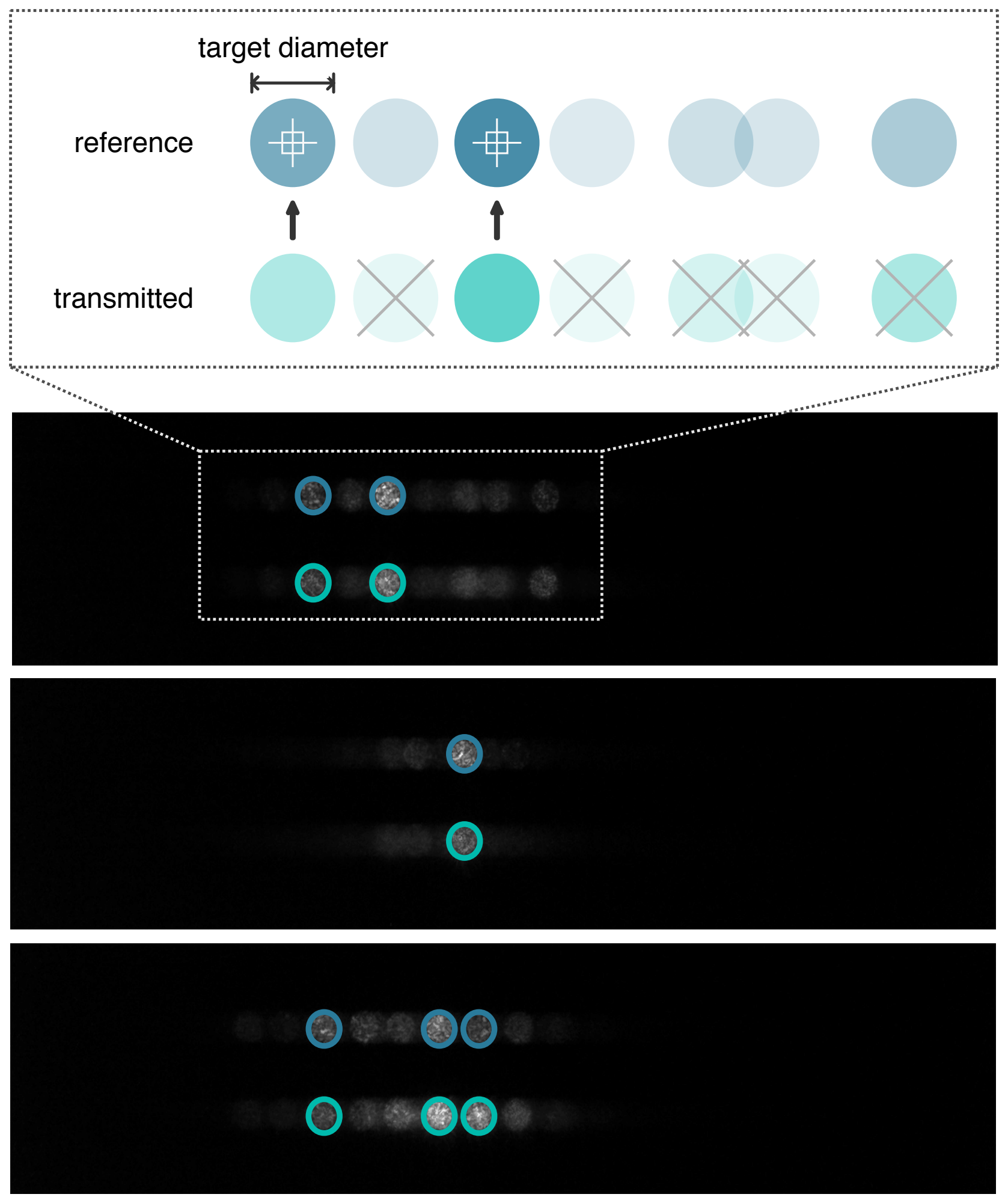
target diameter
reference
transmitted

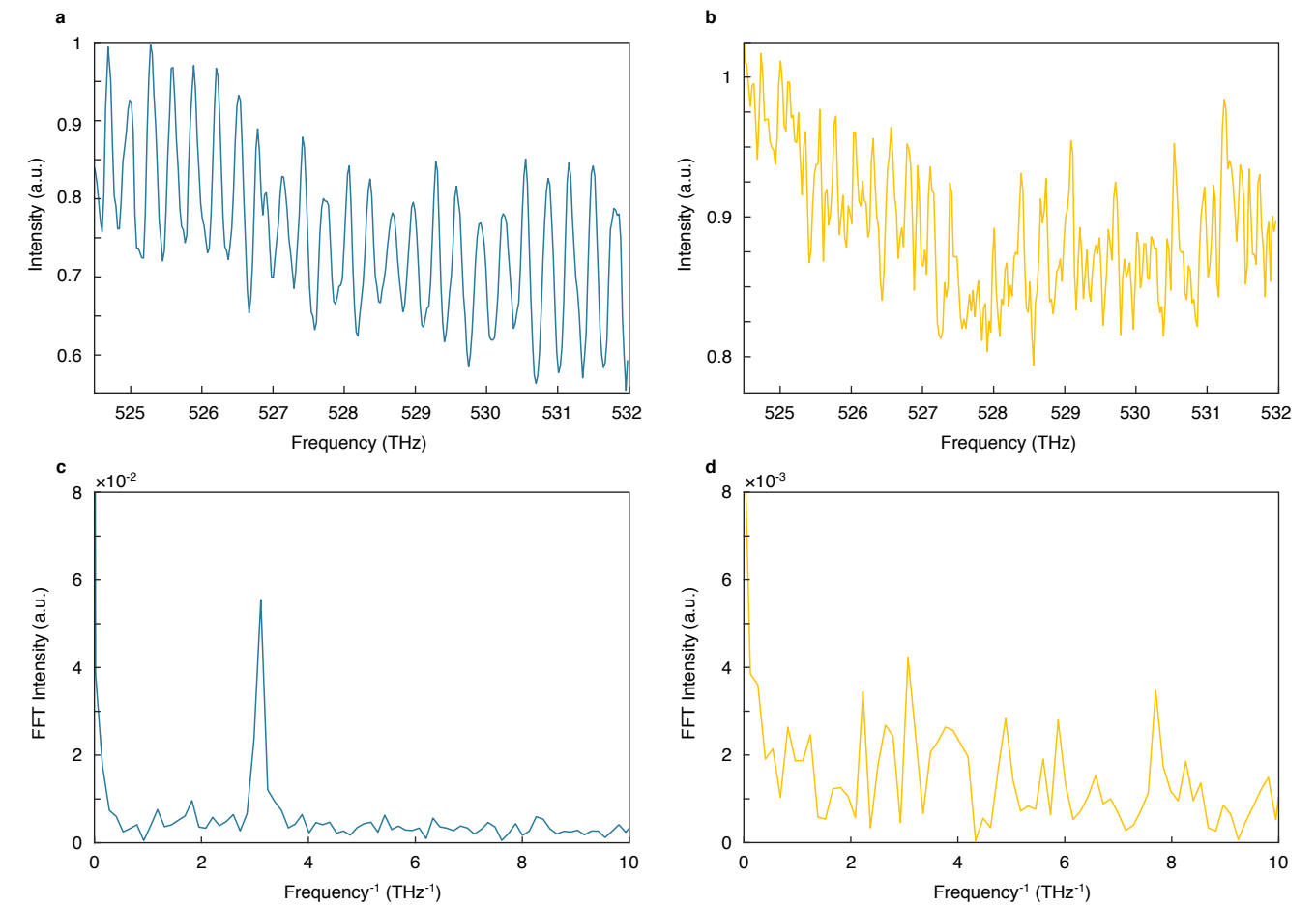
a
Intensity (a.u.)
Frequency (THz)
b
Intensity (a.u.)
Frequency (THz)
c
×10-2
FFT Intensity (a.u.)
Frequency-1 (THz-1)
d
×10-3
FFT Intensity (a.u.)
Frequency-1 (THz-1)